Amino Acids (2011) 41:1113–1122
DOI 10.1007/s00726-010-0769-y

ORIGINAL ARTICLE

Optimization of matrix metalloproteinase fluorogenic probes for osteoarthritis imaging

Ju Hee Ryu · Aeju Lee · Jin Hee Na · Seulki Lee · Hyung Jun Ahn · Jong Woong Park · Cheol-Hee Ahn · Byung-Soo Kim · Ick Chan Kwon · Kuiwon Choi · Inchan Youn · Kwangmeyung Kim

Received: 4 October 2009 / Accepted: 2 September 2010 / Published online: 16 October 2010

Abstract Among the classical collagenases, matrix metalloproteinase-13 (called MMP-13, collagenase-3) is one of the most important components for cartilage destruction of osteoarthritis (OA) developments. Despite many efforts, the detection methods of MMP-13 activity have been met with limited success in vivo, in part, due to the low sensitivity and low selectivity by homology of MMP family. Previously, we demonstrated the use of strongly dark-quenched fluorogenic probe allowed for the visual detection of MMP-13 in vitro and in OA-induced rat models. In this study, we described the optimization of MMP-13 fluorogenic probe for OA detection in vivo. Three candidate probes demonstrated recovered fluorescent intensity proportional with MMP-13 concentrations, respectively; however, Probe 2 exhibited both high signal amplification and selective recognition for MMP-13, not MMP-2 and MMP-9 in vitro. When Probe 2 was applied to OA-induced rat models, clear visualization of MMP-13 activity in OA-induced cartilage was obtained. Optimized MMP-13 fluorogenic probe can be applied to detect and image OA and have potential for evaluating the in vivo efficacy of MMP-13 inhibitors which are being tested for therapeutic treatment of OA.

Keywords Matrix metalloproteinase (MMP) · Osteoarthritis · Fluorogenic probe · Optical imaging · Peptide

J. H. Ryu and A. Lee contributed equally to this paper.

J. H. Ryu · A. Lee · J. H. Na · S. Lee · H. J. Ahn · I. C. Kwon · K. Choi · I. Youn (✉) · K. Kim (✉)
Biomedical Research Center, Korea Institute of Science and Technology, Seongbuk-gu, Seoul, South Korea
e-mail: iyoun@kist.re.kr

K. Kim
e-mail: kim@kist.re.kr

J. W. Park
Department of Orthopaedic Surgery, College of Medicine, Korea University, Danwon-gu, Ansan, Gyeonggi, South Korea

C.-H. Ahn
Department of Materials Science and Engineering, Seoul National University, San 56-1, Sillim-dong, Gwanak-gu, Seoul, South Korea

J. H. Ryu · B.-S. Kim
School of Chemical and Biological Engineering, Seoul National University, San 56-1, Sillim-dong, Gwanak-gu, Seoul, South Korea

Introduction

Proteases are integrally involved in tumor formation, angiogenesis, local invasion and joint diseases (Afjehi-Sadat et al. 2004; Bremer et al. 2001a, b; Takaishi et al. 2008). Among a wide variety of proteolytic enzymes, the matrix metalloproteinase (MMP) family has received much attention (Terp et al. 2002; Watkins et al. 2009). The MMPs are responsible for degradation of a variety of extracellular matrix components in both normal tissue remodeling and pathological states. In particular, elevated levels of MMPs have been found in pathological conditions such as rheumatoid arthritis (Martel-Pelletier et al. 1994), OA (Martel-Pelletier et al. 1994; Marini et al. 2003), and tumor metastasis (Furcht et al. 1994; Stetler-Stevenson et al. 1993) which involve degradation of connective tissue. MMPs are a class of secretory proteinases, including collagenases (MMP-1, -8, and -13), gelatinases (MMP-2, and -9), and stromelysins (MMP-3, -10 and -11), that are classified according to location, structural similarity, and substrate preferences.

In human OA, many MMPs including MMP-1, -2, -3, -7, -8, -9, and -13 are expressed in articular cartilage (Takaishi et al. 2008; Ohuchi et al. 1997). However, type II collagen, a major fibrillar interstitial collagen in cartilage, is extremely resistant to most proteinases because of its triple-helical structure (Knäuper et al. 1996; Mitchell et al. 1996). Thus, only MMPs including the classical collagenases (MMP-1, -8, and -13) can degrade fibrillar collagen for OA (Yamanaka et al. 2000; Yoshihara et al. 2000). Among the classical collagenases, MMP-13 is thought to be the most important for degradation of collagen within the cartilage due to its preferential digestion of type II collagen over type I and III collagens. Recently, many studies demonstrated that the expression pattern of MMP-13 is closely related with cartilage destruction in OA developments (Kamekura et al. 2005). Thus, the excess MMP-13 production in OA offers the possibility for successful MMP-13 targeted OA imaging and also for detection of MMP-13 inhibition for OA treatment.

Preexistent activity assays for MMPs contain methods based on physiological substrates (e.g. radiolabeled collagen, or proteoglycans) or synthetic substrate (Beekman et al. 1996; Knight et al. 1992; Stack and Gray 1989). However, the former methods are mostly too insensitive for detection of MMP activity in vivo. Recently, a variety of fluorogenic probes for measuring activity of protease have been described to measure activity of MMPs (Blum 2008; Bremer et al. 2001a, b; Chen et al. 2005; Liu et al. 2010; Nagase et al. 1994). These fluorogenic probes comprise a fluorophore and a quencher attached to a short amino acid sequence of target enzyme. In a normal state, the emitting light from the fluorophore is absorbed into the quencher by resonance energy transfer. Once target enzymes like MMPs cleave specific peptide substrates, separating fluorophore from the quencher, the extent of fluorescence increases remarkably. Despite many efforts, many of these fluorogenic probes are thus far limited in usefulness in vivo, in part, due to the poor specificity and in vivo stability. The most successful of these efforts has been directed against MMP-2 and MMP-9 (Jiang et al. 2004). However, these probes are cleaved by various other MMPs and even other proteases as well as MMP-2 and MMP-9. That means it is only "more" selective for MMP-2 and MMP-9 compared with other MMPs (Breyholz et al. 2005; Watkins et al. 2009). The MMPs are a homologous family of enzymes in that they possess high sequence similarity and similar three-dimensional structures (Terp et al. 2002). In fact, catalytic domains of MMPs are known to be with sequence similarities in the range 50–88% and identities in the range 33–79% (Sang and Douglas 1996). These properties may hamper MMP probes to be designed highly sensitive and specific. A highly active and selective substrate is essential for in vivo imaging with high resolution.

Previously, we have developed activatable near-infrared fluorescence dark-quenched fluorogenic probe to image MMP-13 activity in vivo (Lee et al. 2008). The use of dark-quenched fluorogenic probe consisting of a pair of a fluorophore (Cy5.5) and a quencher (black hole quencher-3; BHQ-3) showed low fluorescence background and significant fluorescent signal recovery, enabling sensitive visual detection in OA-induced rat model. In this study, we described optimization of MMP-13 fluorogenic probe for OA detection in vivo. We investigated if three candidate probes for OA imaging can make high signal amplification and specific recognition by MMP-13 in vitro. Next, the selected probe was applied to OA-induced cartilage and the fluorescence intensity in OA-induced cartilage was compared with that in normal or inhibitor-treated cartilage. Optimized MMP-13 fluorogenic probe can be applied to detect and image OA and has the potential for evaluating in vivo efficacy of MMP-13 inhibitors which are being tested for therapeutic treatment of OA.

Materials and methods

Materials

Individual peptides were synthesized in Peptron (Daejeon, Korea), purified by reversed-phase high liquid chromatography (RP-HPLC), and characterized by mass spectrometry. Cy5.5 mono-*N*-hydroxysuccinamide ester (Cy5.5-NHS) was purchased from GE Healthcare (Piscateway, NJ), BHQ-3 mono-*N*-hydroxysuccinamide ester (BHQ-3-NHS) from Biosearch Technologies, Inc. (Novato, CA), dimethylformamide (DMF), *N*-methyl morpholine (NMM), trifluoroacetic acid (TFA), anisole and ethyl ether from Sigma, MMP-2, MMP-9, MMP-13 from R&D Systems, Inc. (Minneapolis, MN), MMP-13 inhibitor [pyrimidine-4,6-dicarboxylic acid, bis-(4-fluoro-3-methyl-benzylamide)].

The MMP probe preparation

Three candidate probes and one control probe were prepared by conjugating near-infrared (NIR) fluorophore, Cy5.5 (ex/em; 675/690) and black hole quencher-3 (BHQ-3, abs. 650 nm) to respective MMP substrate peptide (Table 1; Figs. 1, 2a). Peptide for Probe 1 [Gly-*Pro-Leu-Gly-Val-Arg*(Pbf)-Gly-Lys(Boc)-Gly-Gly, substrate site is italicized, the cleavage site between Gly and Val] (Bremer et al. 2001a, b), peptide for Probe 2 [Gly-*Val-Pro-Leu-Ser*(*tBu*)-*Leu-Thr*(*tBu*)-*Met*-Gly-Lys(Boc)-Gly-Gly, substrate site is italicized, the cleavage site between Ser and Leu] (Turk et al. 2001) and peptide for Probe 3 [Gly-*Pro-Leu-Gly-Met-Arg*(Pbf)-*Gly*-Leu-Gly-Lys(Boc)-Gly-Gly, substrate site is

Table 1 Peptide sequence for MMP probes

Probe	Peptide sequence
Probe-Con	G*PL-GMRG*LGK
Probe 1	G*PLG-VR*GKGG
Probe 2	G*VPLS-LTM*GKGG
Probe 3	G*PL-GMRG*LGKGG

The substrate site is italicized and the cleavage site is indicated by a hyphen

italicized, the cleavage site between Leu and Gly] (Deng et al. 2000) were synthesized using standard solid-phase Fmoc peptide chemistry. First, Cy5.5-NHS (8.4 μmol) was coupled to the N terminus of the peptides for Probe 1, Probe 2 and Probe 3 (4.0 μmol) in anhydrous DMF containing NMM (10 μmol) at room temperature in the dark with shaking for 2 h. The Cy5.5-MMP substrate peptide was precipitated by adding ethyl ether. The precipitate was washed with ethyl ether and dried in vaccum. Removal of side chain protecting groups was achieved by incubating in 1 ml of TFA/distillated water (DW)/anisole (95:2.5:2.5, v/v). The TFA was evaporated on the rotary evaporator and an additional 1 ml of DW containing 0.1% TFA/acetonitrile containing 0.1% TFA (1:1, v/v) was then added to the product in the rotary evaporator. The dissolved product in the rotary evaporator was purified by C18 semi-preparative RP-HPLC; 20–90% acetonitrile containing 0.1% TFA versus DW containing 0.1% TFA over 20 min at a flow rate of 4.0 ml/min. Purity (>95%) was confirmed by analytical RP-HPLC. The appropriate fractions were collected and lyophilized. Next, the BHQ-3-NHS (0.90 μmol) was coupled to the primary amine of the lysine of the Cy5.5-MMP substrate peptide (0.90 μmol) in anhydrous DMF containing NMM (3 μmol) at room temperature in the dark with shaking overnight. The product was purified by C18 semi-preparative RP-HPLC; 30–70% acetonitrile containing 0.1% TFA versus DW containing 0.1% TFA over 20 min at a flow rate of 4.0 ml/min. The appropriate fractions were collected and lyophilized. Three candidate probes were characterized by analytical RP-HPLC (Purity >95%), MALDI-TOF mass spectrometry (Probe 1, *m*/*z* calculated: 2326.73, found: 2325; Probe 2, *m*/*z* calculated: 2546.03, found: 2544; Probe 3, *m*/*z* calculated: 2529.01, found: 2526), UV–vis spectra, and emission spectra (Fig. 2b–e).

For conjugation of BHQ-3 to the primary amine of the lysine in the peptide substrate for Probe-Con [Fmoc-Gly-Pro-Leu-Gly-Met-Arg(Pbf)-Gly-Leu-Gly-Lys(Dde)-Resin, substrate site is italicized, the cleavage site between Leu and Gly], the Dde protecting group was selectively removed by addition of 2% hydrazine in DMF (Lee et al. 2008). Dde is removed by 2% hydrazine in DMF within minutes and deprotection of Dde with hydrazine could readily cleave the Fmoc group (Augusjyns et al. 1998). Reaction time with hydrazine was controlled both for selective removal of Dde and no damage to other chemical structure including Fmoc. After extensive washing for the

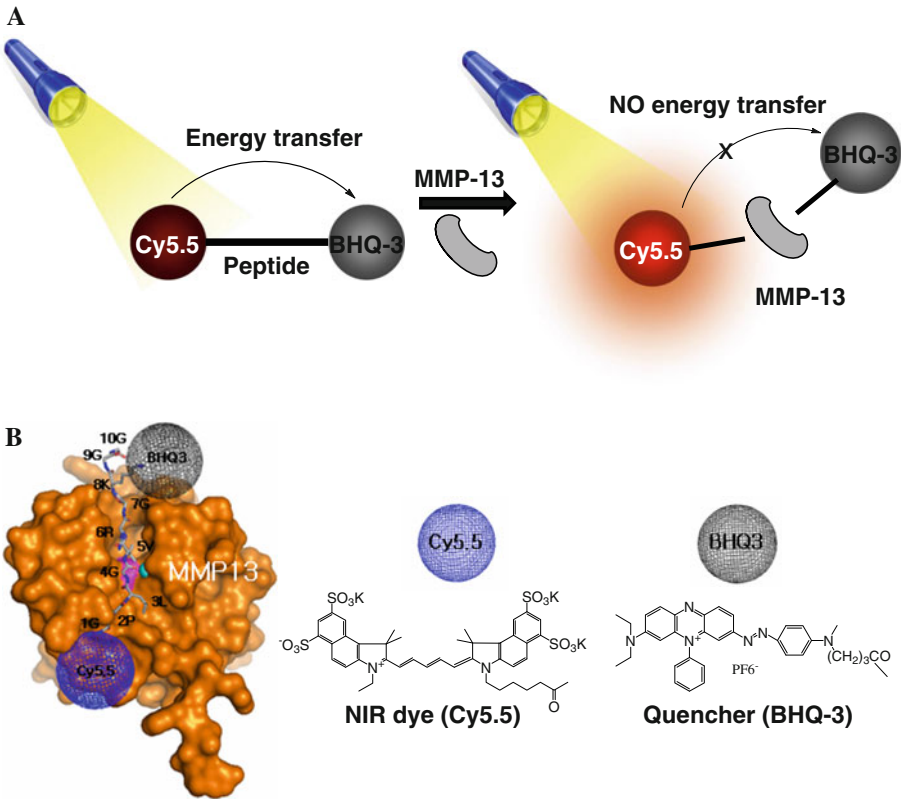

Fig. 1 **a** Schematic diagram of MMP fluorogenic probe. MMP probe is consisted of Cy5.5, BHQ-3 and MMP substrate peptide. MMP probe is quenched before the addition of MMP-13. The addition of MMP-13 causes recovery of NIR fluorescent signals. **b** Accessibility of probe to MMP-13 predicted by modeling. The molecular surface of human MMP-13 and Probe 1 containing peptide substrate and two bulky chemicals, Cy5.5 and BHQ-3, are modeled in the binding pocket. Glutamic acid and Zn ion are located in the binding pocket (glutamic acid: magenta, Zn ion: cyan). Figures were drawn by the program Pymol [DeLano, W.L. The PyMOL Molecular Graphics System (2002) on World Wide Web (http://www.pymol.org)] (color figure online)

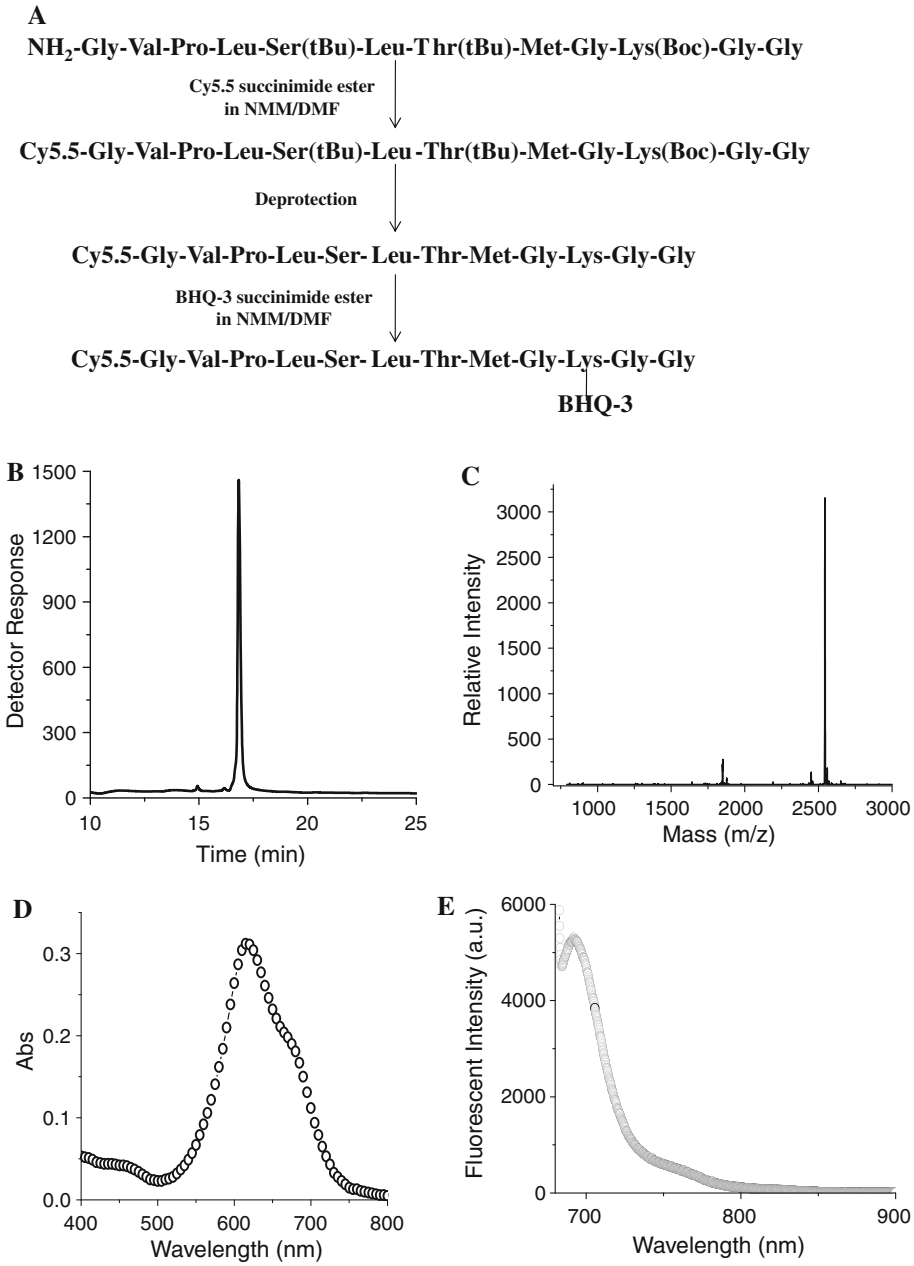

Fig. 2 **a** Synthetic scheme of Probe 2. Analytical experiments including **b** HPLC, **c** MALDI-TOF mass spectrometry, **d** UV–vis spectra, and **e** emission spectra of Probe 2

peptide resin, BHQ-3-NHS in anhydrous DMF was added and reacted overnight. Subsequently, the Fmoc group was removed from the peptide resin and Cy5.5-NHS was conjugated to the N-terminal glycine. After deprotecting and cleaving the peptide from the resin using TFA, resulting Probe-Con was further purified by semi-preparative RP-HPLC and characterized by analytical RP-HPLC (Purity >95%).

Structure-based probe design

The molecular surface of human MMP-13 and three probes containing peptide substrate and two bulky chemicals, Cy5.5 and BHQ-3 are modeled in the binding pocket to predict the accessibility of three probes to MMP-13. From the peptide-bound structures (PDB accession code: 2OY2, 1JAP), we built a model of human MMP-13 using the program O (Jones et al. 1991).

Enzyme specificity of MMP probes

The specificity of the MMP probes was examined by incubating MMP probes (20 nM) in the TCNB buffer (50 mM TRIZMA·HCl, 10 mM $CaCl_2 \cdot 2H_2O$, 0.15 M NaCl, 0.05% Brij35, pH 7.5) containing 15 nM of activated MMP-2, -7, -9, and -13, respectively. MMP-2, -7,

-9 and -13 enzymes were activated by incubating with 2.5 mM of *p*-aminophenyl mercuric acid in 0.1% NaOH buffer for 1 h at 37°C before initiation of the assay. Fluorescence intensity was monitored using a spectrofluorometer (F-7000 Fluorescence Spectrophotometer, Hitach, Tokyo, Japan) every 10 min at 37°C. The excitation wavelength was set at 675 nm and emission spectra recorded from 676 to 800 nm. The same experimental conditions were applied to various concentrations of activated MMP-13 (1.88, 3.75, 7.5, 15, 30 nM) and MMP-13 (15 nM) with MMP-13 inhibitor for three MMP probes in the presence of fixed concentration of MMP probes (20 nM).

OA-induced rat model

Sprague–Dawley rats (250–300 g) were anesthetized with an intramuscular administration of ketamine hydrochloride (90 mg/kg) and xylazine hydrochloride (10 mg/kg). The right and left lower extremities were shaved and prepared for aseptic surgery. After squeezing the leg, a sterile rubber tourniquet was applied for avascular filed during surgery (Kamekura et al. 2005). Under the operating microscope (Leica, M650, USA), the right knee joint was exposed using the anteromedial parapatellar approach. The patellar tendon was transected. Then, the anterior/posterior cruciate ligaments and the medial/lateral collateral ligaments were transected. The medial/lateral menisci were totally menisectomized. After copious irrigation with saline, the knee joint capsule was repaired with an absorbable suture and the skin was closed with a 4-0 monofilament nylon. The animals were allowed unrestricted activity, food, and water ad libitum.

In vivo NIR imaging

Eight weeks after surgery treatment, Probe 2 (10 μg/100 μl/cartilage, 4 nM) was injected into OA-induced and normal cartilages and fluorescence signals in OA-induced and normal cartilages were imaged using in vivo fluorescence tomography, eXplore Optix^{TM} (ART Advanced Research Technologies Inc., Montreal, Canada). For inhibitor-treated rat model, MMP-13 inhibitor was treated into OA-induced cartilage 30 min before probe injection. One hour after MMP probe injection, the fluorescence recovery profiles in OA-induced and normal cartilages were imaged by positioning rats on an animal plate heated to 36°C in the eXplore Optix System. Laser power and count time settings were optimized 13 μW and 0.3 s per point. Excitation and emission spots were raster-scanned in 1 mm step over the selected region of interest to generate emission wavelength scan. A 670 nm pulsed laser diode was used to excite Cy5.5. NIR fluorescence emission at 700 nm was collected and detected with a fast photomultiplier tube (Hamamatsu, Japan) and a single photon counting system (Becker and Hickl GmbH, Berlin, Germany). Quantitative data are calculated using the region of interest function of Analysis Workstation software (ART Advanced Research Technologies Inc., Montreal, Canada), and values are presented as mean ± SE for groups of three animals.

Histological analysis

To compare the destruction of OA and normal cartilages, the whole knee joints were dissected, and fixed in 4% (v/v) paraformaldehyde buffered with PBS (pH 7.4) for 4 h at 4°C. Specimens were dehydrated with a series of graded alcohol, and embedded in paraffin. Tissue sections (5 μm thick) were cut from the joints. Sections were stained with Safranin-O-fast green (Kamekura et al. 2005).

Results and discussion

Preparation of three MMP fluorogenic probes

Three candidate probes and one control probe were prepared by conjugating NIR fluorophores (Cy5.5) and quencher (BHQ-3) to known MMP peptide sequences (Table 1; Figs. 1, 2a). Probe-Con, used in previous study where Probe-Con enabled sensitive visual detection of MMP-13 activity in OA-induced rat model, was synthesized to evaluate fluorescence amplification capacity of three candidate probes. The probe preparation was undertaken considering that two bulky chemicals, Cy5.5 and BHQ-3 of probes may adversely affect recognition of the peptide sequence by MMP-13, resulting in decreased cleavage rate. Previously, the fluorogenic probe containing short peptide, Cy5.5 and BHQ-3, was predicted to fail to access the binding pocket of human MMP-13 by modeling (Lee et al. 2008). However, the incorporation of several amino acid sequences enables effective binding of the fluorogenic probe to binding pocket. Thus, we evaluated whether two bulky chemicals, Cy5.5 and BHQ-3, of probes hamper recognition of the peptide sequence by MMP-13 in three candidate probes using computer modeling. The molecular surface of human MMP-13 and three candidate probes containing peptide substrate and two bulky chemicals, Cy5.5 and BHQ-3, are modeled in the binding pocket (Fig. 1b). The designed MMP probes were predicted to achieve an effective binding to MMP-13, which may be attributed to incorporated amino acid sequences (Probes 1 and 2: glycine and glycine-lysine-glycine-glycine, Probe 3: glycine and leucine-glycine-lysine-glycine-glycine).

Specificity of MMP probes to various MMPs

Incubation of MMP probes with MMP-13 showed significant increase of the fluorescent signals (at 690 nm) over time (Fig. 3a) in vitro. In vitro assay can afford a tool for rapid and continuous measurement and be performed using a relatively small amount of probes. The initial concentration of probes was set to 20 nM. Probes (20 nM, before activation) have the similar value in UV–vis spectra and emission spectra. Three MMP probes were almost completely quenched before treatment of MMPs, resulting in significantly lower fluorescent backgrounds. Approximately 32-, 36-, 6-fold increases in fluorescence intensity occur in the Probe 1, Probe 2, Probe 3 samples after 80 min of incubation, respectively (22-fold increase in the Probe-Con sample). Probe 3 includes glycine-glycine in C-terminal of peptide sequence of Probe-Con, and was synthesized using different method compared to Probe-Con, which made significant reduction in fluorescent intensity recovery in vitro. When three MMP probes were treated with various concentrations of activated MMP-13, recovered fluorescent intensity demonstrated the proportional relationship with MMP-13 concentrations, respectively (Fig. 3b). Recovered fluorescent intensities had linear relationship with MMP-13 concentrations up to 1.88 nM in the Probe 1 ($R^2 = 0.999$) and Probe 2 ($R^2 = 0.999$), whereas up to 7.5 nM in the Probe 3 ($R^2 = 0.958$).

To select the optimized MMP probe for OA imaging, the specificity of three MMP probes was examined in vitro after treatment MMP-2, -7, -9 and -13. The fluorescence intensity was compared after cleavage of three MMP probes via MMP-2, -7, -9 and -13, respectively. Various MMPs were detected during OA development, including MMP-1, -2, -7, -8, -9 and -13. However, MMP-13 is key factor for cartilage destruction comparison with MMP-1 and -8 in OA development. Thus, optimized MMP probe for OA imaging should have specificity for MMP-13, not other MMPs. Furthermore, MMP-2 and -9 are not only over-expressed in several types of cancer but also angiogenesis which induce wrong diagnosis for OA (Bremer et al. 2001a, b; Himelstein et al. 1994–1995). MMP-7 was reported to be highly expressed in OA articular cartilage and play an important role in the extracellular matrix degradation of the OA cartilage (Ohta et al. 1998). Thus, high specificity for MMP-7 could be advantageous to OA imaging. The fluorescence intensity was significantly amplified when MMP-13 was added in Probes 1 and 2, respectively (Fig. 3c). In addition, Probe 2 showed significantly amplified recovery of fluorescence intensity in the sample treated by MMP-13 and -7 and a small amount of recovery of fluorescence intensity in the samples treated by MMP-2 and -9, whereas Probe 1 demonstrated significantly amplified recovery of fluorescence intensity in samples treated by MMP-2 and -9 as well as that treated by MMP-13. Probe 3 demonstrated a small amount of recovery of the NIR fluorescent intensity in all samples treated by MMP-2, -7, -9 and -13. Probe-Con showed significantly amplified recovery of fluorescence intensity in samples treated by MMP-2 and -13. These results suggest that Probe 2 is cleaved effectively by MMP-13 and specific to MMP-13 compared to other tested MMP probes. Therefore, to achieve an efficient OA imaging, where MMP-13 expression is critical, we chose Probe 2 as the fluorogenic MMP probe for OA imaging.

Probe-Con has similar MMP specificity with Probe 3; however, higher reactivity for several MMPs than Probe 3, as seen in Fig. 3c. Probe 3 has the same sequence as Probe-Con except that the former has two glycine residues. Two glycine residues were incorporated into three candidate probe sequences for further modification through C-terminal of peptide sequence. Spacer arm such as two glycine residues can overcome the steric hindrance in the interaction between the active peptide sequence and its target (Chan et al. 2007; Chang et al. 2005; Massaguer et al. 2001). However, simple incorporation of two glycine residues is not enough to explain why reactivity of Probe 3 toward MMPs reduced, so its reason should be studied by further experiment using modeling.

Animal optical imaging

A rat OA model was created by ligament transection and meniscectomy. Eight weeks after surgery treatment, histological analyses in OA-induced cartilage indicated that the cartilage was lost severely and the bone–cartilage interface was altered significantly in all animals (Fig. 4a), which means severe degeneration of cartilage. On the other hand, the histological section of the normal cartilage exhibited well-maintained structure of the cartilage layer and regular cartilage surface.

Eight weeks after surgery treatment, we investigated the potential use of Probe 2 in OA-induced rat model using in vivo fluorescence tomography (eXplore Optix^{TM}) (Fig. 4c). Twenty minutes and 1 h after Probe 2 injection into OA-induced and normal cartilages, respectively, NIR fluorescence signal was monitored. Probe 2 provided intense fluorescence signal in OA-induced cartilage, whereas fluorescence signal was weak in normal cartilage 1 h after probe injection. In addition, the fluorescence signal in OA-induced cartilage was highly reduced when MMP-13 inhibitor was treated into OA-induced cartilage 30 min before the probe injection. The FL intensity in OA-induced cartilage increased over time, while that in normal cartilage and inhibitor-treated cartilage kept at the same low level over time. Fluorescence signals of Probe 2 for OA-induced and normal cartilages 1 h after probe injection

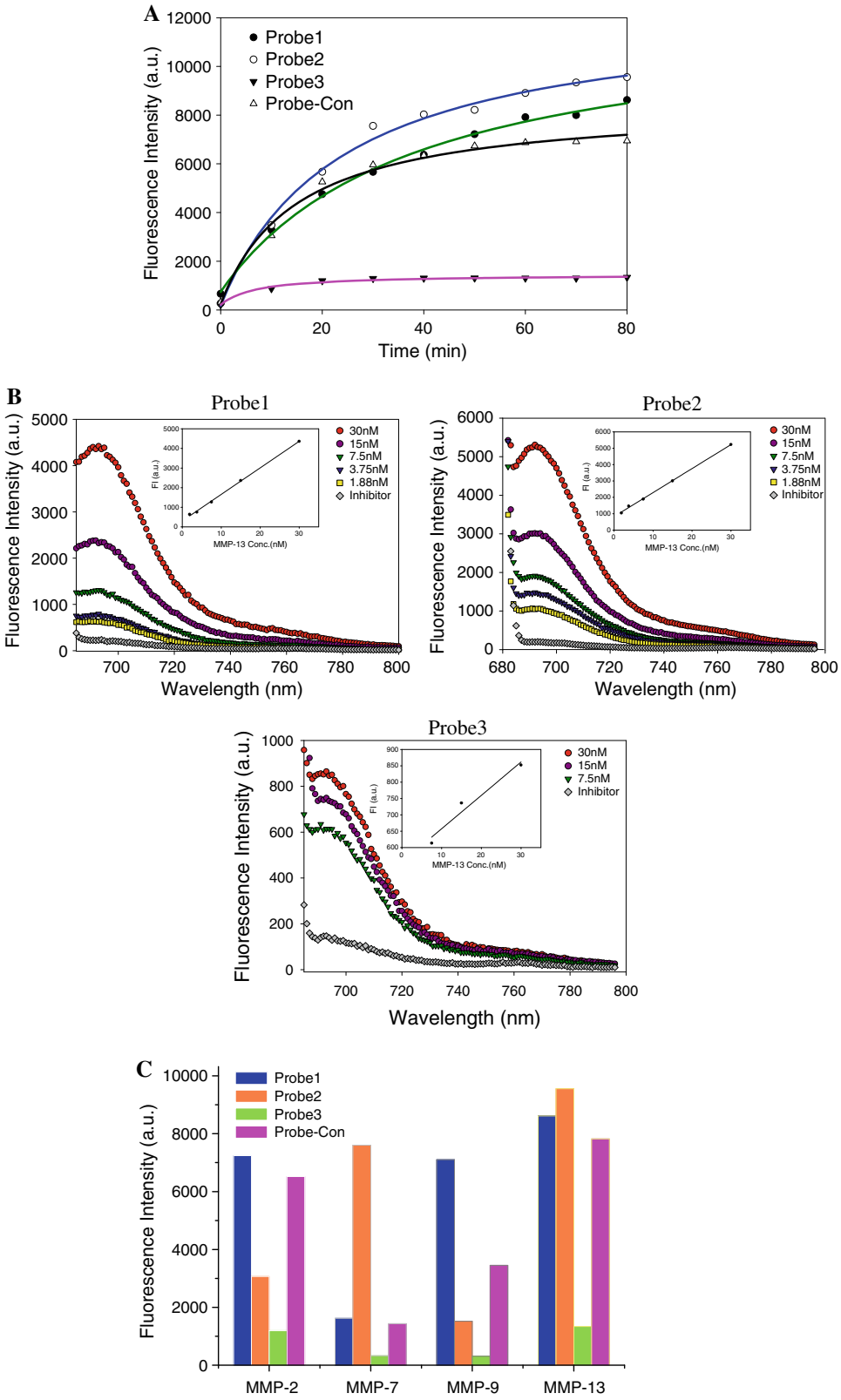

Fig. 3 **a** Recovery of NIR fluorescence intensities of MMP probes (20 nM) in the presence of MMP-13 (15 nM) as a function of time following incubation for 80 min at 37°C. **b** Fluorescence emission spectra of MMP probes in the presence of various concentrations of MMP-13 following incubation for 20 min at 37°C; *inset* MMP-13 standard curve. **c** Fluorescence intensity of three candidate probes and Probe-Con (20 nM) in the presence of MMP-2, -7, -9, and -13 (15 nM) for 80 min at 37°C

were quantified by total photon counts in the cartilages. Total photon counts of OA-induced and normal cartilages were $(9.3 \pm 1.3) \times 10^6$ and $(2.4 \pm 0.8) \times 10^6$, respectively, which indicates that the NIR fluorescence intensity in the OA-induced cartilage was 3.8-fold higher than that in the normal cartilage (Fig. 4b). On the other

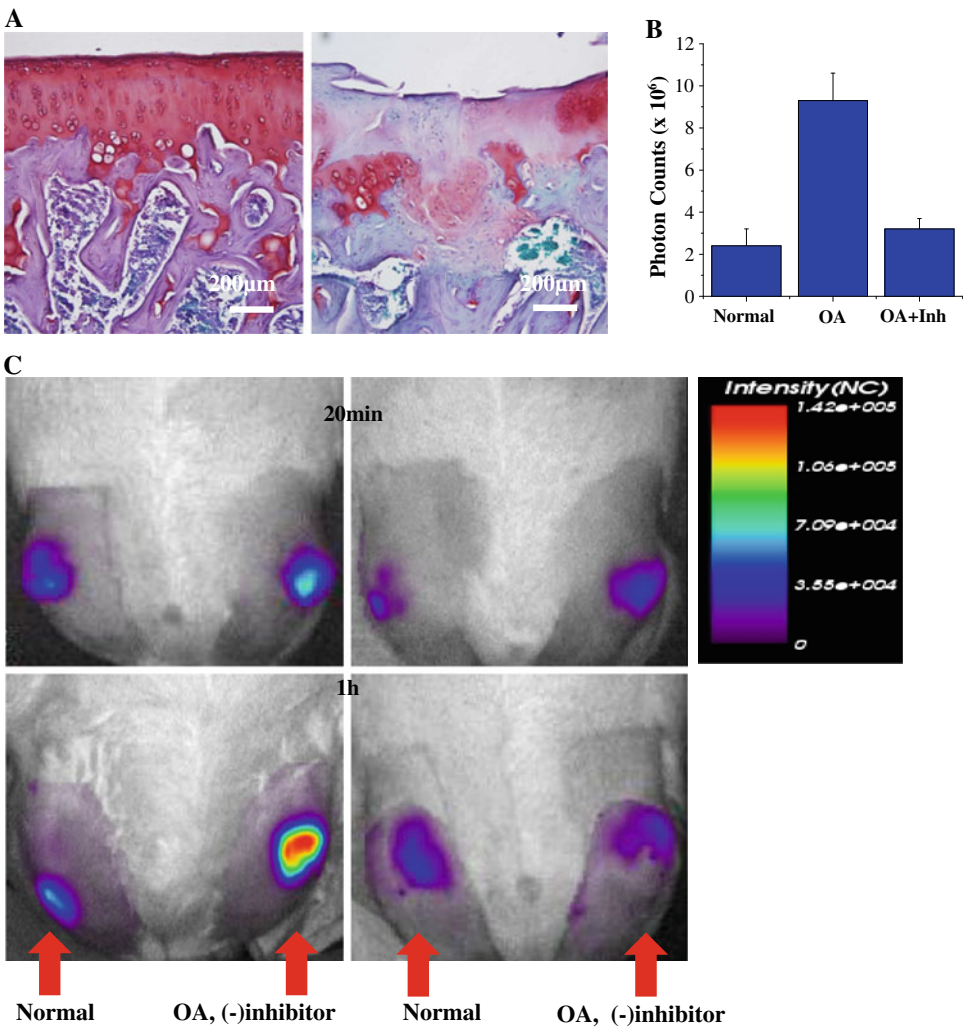

Fig. 4 **a** Histological analysis of normal (*right*) and OA (*left*) joints by Safranin-O staining. **b** Total photon counts in normal, OA-induced and OA-induced and inhibitor-treated cartilages. **c** In vivo NIR fluorescence tomographic images of normal and OA cartilages 20 min and 1 h after cartilage injection of Probe 2 with or without addition of MMP-13 inhibitor in OA-induced rat model. *Left* Probe 2 without MMP-13 inhibitor. *Right* Probe 2 with MMP-13 inhibitor

hand, total photon counts of inhibitor-treated cartilage were significantly reduced $(3.2 \pm 0.5) \times 10^6$. Taken together, these results demonstrate that Probe 2 could monitor MMP-13 activity in vivo, which enabled effective OA imaging.

Although fluorogenic MMPs probes are promising candidates as various disease-selective imaging probes, the detection methods of MMP-13 activity have met with limited success in vivo. The first reason is low selectivity against MMP-13 for OA imaging under in vivo condition, i.e. due to the homologous of MMP family. Desired MMP probes should be sensitive to targeted MMP, not other MMP family. Preexistent MMP probes have "more" sensitive to desired MMP compared with other MMP family. Thus, herein, we optimized the MMP probes for MMP-13 for OA imaging. The second reason is low sensitivity of fluorogenic probe for in vivo application. Optical imaging is limited to only few millimeter-depth observations such as for small animal models or superficial tissues of human, because components of a tissue absorb fluorescent light. We could envision improvements of imaging probe to monitor fluorescence showing the presence of target molecules in a deeper tissue of human. We anticipate that our newly devised fluorogenic probe is simple but highly efficient so it could be a good candidate probe used to detect human OA and monitor therapy.

Conclusion

In summary, we have reported the optimization of MMP-13 fluorogenic probe for the active and selective detection of OA in vitro and in vivo. Among three candidate probes, Probe 2 with GVPLS-LTMGKGG peptide sequence demonstrated high signal amplification and selective recognition for MMP-13, not MMP-2 and MMP-9 in vitro. Moreover, Probe 2 exhibited intense signal amplification in OA-induced cartilage in vivo. Consequently, optimized MMP-13 fluorogenic probe has great potential for use in diagnosis of OA without wrong diagnosis from other MMPs related physiological condition or disease.

Additionally, optical probe used in this study can be extended to other proteases simply by changing the specific peptide substrate linker between the fluorophore and quencher. For more specific OA imaging, optimization of the probe substrate should be continuously researched. In addition, other methods such as the use of several kinds of probes together can be applicable.

Acknowledgments This work was financially supported by the Real-Time Molecular Imaging Project, GRL program, and the Pioneer Research Program for Covering Technology of MEST and by a grant to the Intramural Research Program (Theragnosis) of the KIST, and by a grant (A062254) of the Korea Health 21 R&D Project.

Conflict of interest The authors declare that they have no conflict of interest.

References

Afjehi-Sadat L, Gruber-Olipitz M, Felizardo M, Slavc I, Lubec G (2004) Expression of proteasomal proteins in ten different tumor cell lines. Amino Acids 27:129–140

Augusjyns K, Kraas W, Jung G (1998) Investigation on the stability of the Dde protecting group used in peptide synthesis: migration to an unprotected lysine. J Pept Res 51:127–133

Beekman B, Drijfhout JW, Bloemhoff W, Ronday HK, Tak PP, te Koppele JM (1996) Convenient fluorometric assay for matrix metalloproteinase activity and its application in biological media. FEBS Lett 390:221–225

Blum G (2008) Use of fluorescent imaging to investigate pathological protease activity. Curr Opin Drug Discov Dev 11:708–716

Bremer C, Tung CH, Weissleder R (2001a) In vivo molecular target assessment of matrix metalloproteinase inhibition. Nat Med 7:743–748

Bremer C, Bredow S, Mahmood U, Weissleder R, Tung CH (2001b) Optical imaging of matrix metalloproteinase-2 activity in tumors: feasibility study in a mouse model. Radiology 221:523–529

Breyholz HJ, Schäfers M, Wagner S, Höltke C, Faust A, Rabeneck H, Levkau B, Schober O, Kopka K (2005) C-5-disubstituted barbiturates as potential molecular probes for noninvasive matrix metalloproteinase imaging. J Med Chem 48:3400–3409

Chan L, Cross HF, She JK, Cavalli G, Martins HFP, Neylon C (2007) Covalent attachment of proteins to solid supports and surfaces via sortase-mediated ligation. PLoS ONE 11:e1164

Chang E, Miller JS, Sun J, Yu WW, Colvin VL, Drezek R, West JL (2005) Protease-activated quantum dot probes. Biochem Biophys Res Commun 334:1317–1321

Chen J, Tung CH, Allport JR, Chen S, Weissleder R, Huang PL (2005) Near-infrared fluorescent imaging of matrix metalloproteinase activity after myocardial infarction. Circulation 111:1800–1805

Deng SJ, Bickett DM, Mitchell JL, Lambert MH, Blackburn RK, Carter HL 3rd, Neugebauer J, Pahel G, Weiner MP, Moss ML (2000) Substrate specificity of human collagenase 3 assessed using a phage-displayed peptide library. J Biol Chem 275:31422–31427

Furcht LT, Skubitz AP, Fields GB (1994) Tumor cell invasion, matrix metalloproteinases, and the dogma. Lab Invest 70:781–783

Himelstein BP, Canete-Soler R, Bernhard EJ, Dilks DW, Muschel RJ (1994–1995) Metalloproteinases in tumor progression: the contribution of MMP-9. Invasion Metastasis 14:246–258

Jiang T, Olson ES, Nguyen QT, Roy M, Jennings PA, Tsien RY (2004) Tumor imaging by means of proteolytic activation of cell-penetrating peptides. Proc Natl Acad Sci USA 101:17867–17872

Jones TA, Zou JY, Cowan SW, Kjeldgaard M (1991) Improved methods for building protein models in electron density maps and the location of errors in these models. Acta Crystallogr A 47:110–119

Kamekura S, Hoshi K, Shimoaka T, Chung U, Chikuda H, Yamada T, Uchida M, Ogata N, Seichi A, Nakamura K, Kawaguchi H (2005) Osteoarthritis development in novel experimental mouse models induced by knee joint instability. Osteoarthritis Cartilage 13:632–641

Knäuper V, Will H, López-Otin C, Smith B, Atkinson SJ, Stanton H, Hembry RM, Murphy G (1996) Cellular mechanisms for human procollagenase-3 (MMP-13) activation. Evidence that MT1-MMP (MMP-14) and gelatinase a (MMP-2) are able to generate active enzyme. J Biol Chem 271:17124–17131

Knight CG, Willenbrock F, Murphy G (1992) A novel coumarin-labelled peptide for sensitive continuous assays of the matrix metalloproteinases. FEBS Lett 296:263–266

Lee S, Park K, Lee SY, Ryu JH, Park JW, Ahn HJ, Kwon IC, Youn IC, Kim K, Choi K (2008) Dark quenched matrix metalloproteinase fluorogenic probe for imaging osteoarthritis development in vivo. Bioconjug Chem 19:1743–1747

Liu TW, Chen J, Zheng G (2010) Peptide-based molecular beacons for cancer imaging and therapy. Amino Acids. doi:10.1007/s00726-010-0499-1

Marini S, Fasciglione GF, Monteleone G, Maiotti M, Tarantino U, Coletta M (2003) A correlation between knee cartilage degradation observed by arthroscopy and synovial proteinases activities. Clin Biochem 36:295–304

Martel-Pelletier J, McCollum R, Fujimoto N, Obata K, Cloutier JM, Pelletier JP (1994) Excess of metalloproteases over tissue inhibitor of metalloprotease may contribute to cartilage degradation in osteoarthritis and rheumatoid arthritis. Lab Invest 70:807–815

Massaguer A, Haro I, Alsina MA, Reig F (2001) Synthesis of RGD containing peptides. Comparative study of their incorporation to the surface of 5-fluoruridine loaded liposomes. J Liposome Res 11:103–113

Mitchell PG, Magna HA, Reeves LM, Lopresti-Morrow LL, Yocum SA, Rosner PJ, Geoghegan KF, Hambor JE (1996) Cloning, expression, and type II collagenolytic activity of matrix metalloproteinase-13 from human osteoarthritic cartilage. J Clin Invest 97:761–768

Nagase H, Fields CG, Fields GB (1994) Design and characterization of a fluorogenic substrate selectively hydrolyzed by stromelysin 1 (matrix metalloproteinase-3). J Biol Chem 269:20952–20957

Ohta S, Imai K, Yamashita K, Matsumoto T, Azumano I, Okada Y (1998) Expression of matrix metalloproteinase 7 (Matrilysin) in human osteoarthritic cartilage. Lab Invest 78:79–87

Ohuchi E, Imai K, Fujii Y, Sato H, Seiki M, Okada Y (1997) Membrane type 1 matrix metalloproteinase digests interstitial collagens and other extracellular matrix macromolecules. J Biol Chem 272:2446–2451

Sang QA, Douglas DA (1996) Computational sequence analysis of matrix metalloproteinases. J Protein Chem 15:137–160

Stack MS, Gray RD (1989) Comparison of vertebrate collagenase and gelatinase using a new fluorogenic substrate peptide. J Biol Chem 264:4277–4281

Stetler-Stevenson WG, Aznavoorian S, Liotta LA (1993) Tumor cell interactions with the extracellular matrix during invasion and metastasis. Annu Rev Cell Biol 9:541–573

Takaishi H, Kimura T, Dalal S, Okada Y, D'Armiento J (2008) Joint diseases and matrix metalloproteinases: a role for MMP-13. Curr Pharm Biotechnol 9:47–54

Terp GE, Cruciani G, Christensen IT, Jørgensen FS (2002) Structural differences of matrix metalloproteinases with potential implications for inhibitor selectivity examined by the GRID/CPCA approach. J Med Chem 45:2675–2684

Turk BE, Huang LL, Piro ET, Cantley LC (2001) Determination of protease cleavage site motifs using mixture-based oriented peptide libraries. Nat Biotechnol 19:661–667

Watkins GA, Jones EF, Scott Shell M, VanBrocklin HF, Pan MH, Hanrahan SM, Feng JJ, He J, Sounni NE, Dill KA, Contag CH, Coussens LM, Franc BL (2009) Development of an optimized activatable MMP-14 targeted SPECT imaging probe. Bioorg Med Chem 17:653–659

Yamanaka H, Matsuda Y, Tanaka M, Sendo W, Nakajima H, Taniguchi A, Kamatani N (2000) Serum matrix metalloproteinase 3 as a predictor of the degree of joint destruction during the six months after measurement, in patients with early rheumatoid arthritis. Arthritis Rheum 43:852–858

Yoshihara Y, Nakamura H, Obata K, Yamada H, Hayakawa T, Fujikawa K, Okada Y (2000) Matrix metalloproteinases and tissue inhibitors of metalloproteinases in synovial fluids from patients with rheumatoid arthritis or osteoarthritis. Ann Rheum Dis 59:455–461